Synthetic Metals, 3 (1981) 111 - 122

OPTICAL REFLECTION STUDIES OF THE ELECTRONIC PROPERTIES OF STAGES 2 - 5 GRAPHITE–$SbCl_5$

P. C. EKLUND, D. S. SMITH and V. R. K. MURTHY

Department of Physics & Astronomy, University of Kentucky, Lexington, KY 40506 (U.S.A.)

(Received June 16, 1980)

Summary

We have measured the absolute reflectance spectra at near-normal incidence for well-characterized stages 2, 3, 4 and 5 graphite–$SbCl_5$. The measurements were made with a prism monochromator in the range 0.1 - 3.0 eV. Because of the air stability of these compounds we have also been able to determine experimentally the values of the real and imaginary parts of the dielectric constant at 1.96 eV by measuring the absolute reflectance of the samples in air and CCl_4 using a He–Ne laser.

The reflectance spectra were analyzed in terms of a phenomenological dielectric constant model with contributions from the core, free carriers, and interband transitions. Interband transitions are modeled as Lorentz oscillators. The spectra were fitted with the additional constraint that the calculated values of the real and imaginary dielectric constant at 1.96 eV matched those directly determined by experiment. The data are discussed in terms of the band model of Blinowski *et al.* and the more recent band model reported by Dresselhaus and Leung.

1. Introduction

In this paper we present the results of an optical reflection study of stages 2 - 5 graphite–$SbCl_5$ in the photon energy range 0.1 - 3.0 eV. The energy region below 0.5 eV, for which little data presently exist, contains a structure which should be reconciled with a band structure model for these compounds.

We have analyzed our spectra in terms of a phenomenological dielectric constant containing contributions from free carriers, interband transitions, and higher energy (core) processes. Interband absorption is either accounted for by the addition of individual Lorentz oscillators into the expression for the dielectric constant, or by the addition of a *group* of narrow Lorentz oscillators which more nearly represents a band of transitions exhibiting a sharp, low-energy threshold for absorption. This low energy threshold can, in principle, be used to locate the Fermi level.

Our calculated values for the real and imaginary parts of the dielectric constant at 1.96 eV are required to be consistent with those determined from near-normal reflectance measurements made on samples submerged in air and CCl_4; these experimentally determined values represent the first reported direct measurements of the optical dielectric constants of a graphite intercalation compound.

Previous optical reflection studies [1 - 6] have clearly shown the existence of sharp Drude edges in stages 1, 2, and 3 donor and acceptor compounds. The spectra in most of these studies [1 - 5] have been analyzed in terms of a conventional Drude model for the dielectric constant with the addition of a frequency-independent imaginary term to account for important low energy interband transitions. These analyses were clearly aimed at extracting the Drude parameters (plasma frequency ω_p and relaxation time τ) from a simple analysis of the shape of the dominant Drude edges in the various spectra. Although we have not analyzed any earlier published data in terms of our more complete dielectric constant model, we have found that for graphite–$SbCl_5$ the more complete analysis generally results in lower plasma frequencies.

Blinowski *et al.* [6] have recently published a direct calculation of the optical dielectric constants in stages 1 and 2 acceptor compounds (based on their quasi-two-dimensional energy band model) and fit their theory to reflectance spectra of several acceptor compounds. Subsequently, Blinowski and Rigaux [7] have proposed a quasi-2D band model for stages 3 and 4 compounds, and Dresselhaus and Leung [8] have reported on a 3D phenomenological band model for stages 1 - 7. In this paper we also briefly comment on these band structures and their connection with our data. A more detailed discussion regarding the relation of their band models to our data will appear in a later publication.

2. Experimental

The samples were prepared by reacting highly-oriented pyrolytic graphite (HOPG) with the vapors of $SbCl_5$, using a two bulb technique. The details of the sample preparation and the air stability of the samples have been reported elsewhere [9]. In spite of the air stability of these compounds, the reflectance spectra were taken on freshly cleaved *c*-faces under flowing, dry nitrogen. A microprocessor controlled, single-beam, prism monochromator with a CaF_2 prism was used to acquire the spectra [10]. The absolute reflectance, R, of a sample was calculated from the ratio of successive single beam reflection spectra of the sample and a freshly evaporated silver mirror. The incident and reflected optical beams made an angle of $\sim 6°$ with respect to the sample *c*-axis. By carefully substituting the standard mirror for the sample, spurious structure due to water vapor absorption was reduced to values of $\Delta R < 0.01$.

Proper staging was confirmed using a four-circle diffractometer and Mo Kα radiation. Samples were selected for reflectance measurements which had no discernible shoulders on the main (00*l*) diffraction peaks. Our values for the stage-dependent, *c*-axis repeat distances are given by $I_c = 6.02 + 3.35n$ for stage number $n \geqslant 2$. This result is in excellent agreement with the literature [11, 12]. In Fig. 1, we show the (00*l*) diffractograms of stages 2 - 5 samples out to $2\theta \sim 50°$.

The samples used in this study also displayed the expected characteristic Raman-doublet at $\sim 1600\ cm^{-1}$ [13]. This doublet is associated with the Γ-pt. phonons in interior and bounding graphitic layers. Because both optical experiments probe comparable skin depths, the Raman data support our contention that the optical depth of the sample is representative of a well-staged sample. Several samples, all of the same nominal stage as determined from X-ray diffraction data, were measured to ensure that the reflectance spectra reported herein are, indeed, representative of pure stage $SbCl_5$–graphite compounds.

Experimental values for the real and imaginary parts of the dielectric constant at 1.96 eV (6328 Å) were determined from the near-normal reflectance of the samples measured in air and in CCl_4. These absolute reflectance measurements were made using a sharply focused (~0.5 mW) He

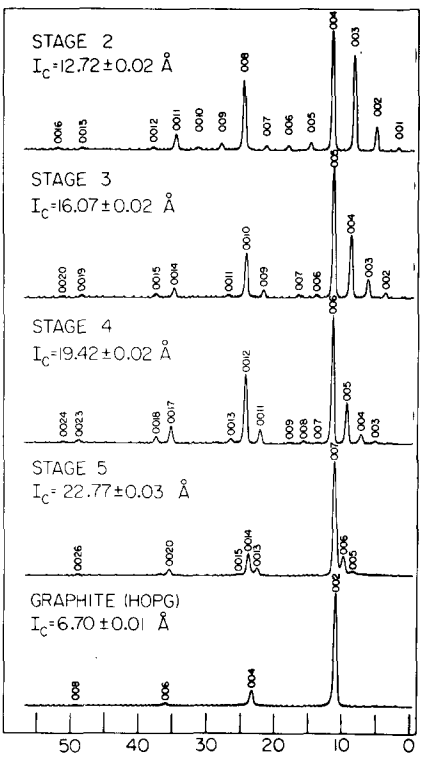

Fig. 1. X-ray data of the (00*l*) diffraction peaks of stage 2 - 5 $SbCl_5$–graphite and HOPG.

He–Ne laser and a Si(pin) detector. A random error of ±0.2% in the absolute reflectance was measured which corresponds to one standard deviation from the average value. Great care was exercised to avoid systematically losing light from the partially diffuse surfaces of the samples. The optical constants n and k of the intercalation compounds were determined from the well known expression for the absolute, near-normal reflectance, R, of a sample submerged in a medium of refractive index n_0,

$$R = \frac{(n - n_0)^2 + k^2}{(n + n_0)^2 + k^2}. \tag{1}$$

By measuring R with the sample submerged in either CCl_4 ($n_0 = 1.460$) or air ($n_0 = 1$), two equations of the form of eqn. (1) are obtained and can be solved for n and k. The real (ϵ_1) and imaginary (ϵ_2) parts of the dielectric constant are, in turn, calculated according to $\epsilon_1 = n^2 - k^2$ and $\epsilon_2 = 2nk$. Our results for the measured values of ϵ_1 and ϵ_2 at 1.96 eV are plotted as a function of reciprocal stage number in Fig. 2(a) and (b). The data show that $\epsilon_1 \approx 4$ and is independent of stage, whereas $\epsilon_2 \approx 8$ for HOPG and falls off roughly linearly with reciprocal stage, as shown in the Figure. Our experimental values for HOPG are in good agreement with those obtained by Taft and Phillip [14] who performed a Kramers–Kronig analysis of near-normal reflectance data covering a wide energy range. The absolute reflectance data taken in air with the He–Ne laser were also used to normalize the spectra acquired with the prism monochromator.

3. The phenomenological, dielectric-constant model

The reflectance at near-normal incidence can be related to the complex dielectric constant, ϵ_*, of the material *via* eqn. (1) and the relation $\epsilon_* = n_*^2$,

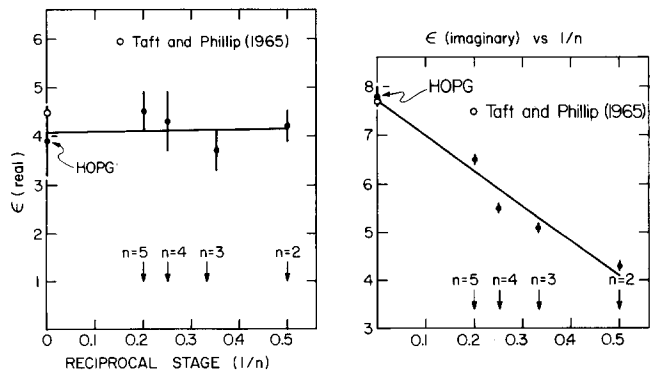

(a) (b)

Fig. 2. (a) ϵ (real) *vs.* Reciprocal stage number ($1/n$) for stage 2 - 5 $SbCl_5$–graphite and HOPG ($n = \infty$). These values were determined from direct measurements of the absolute reflectance of the samples submerged in air and CCl_4. (b) ϵ (imag.) *vs.* Reciprocal stage number ($1/n$). See the caption for (a).

where n_* is the complex, refractive index. The complex dielectric constant of G.I.C.'s in our energy range (0.1 - 3.0 eV) should contain important contributions from free carriers (ϵ_{free}), interband transitions (ϵ_{inter}), and higher energy core processes (ϵ_{core}),

$$\epsilon_* = \epsilon_{\text{core}} + \epsilon_{\text{free}} + \epsilon_{\text{inter}}. \tag{2}$$

Values for the core dielectric constant are real. The expression for the free carrier contribution ϵ_{free} is given in the usual Drude form by

$$\epsilon_{\text{free}}(\omega) = 1 - \frac{(\omega_p/\omega)^2}{1 + i/\omega\tau} \tag{3}$$

where ω_p is the plasma frequency and τ equals the carrier relaxation time. Interband transitions are described in terms of Lorentz oscillators. The contribution to the dielectric constant from a single Lorentz oscillator of frequency ω_j, width Γ_j and strength f_j is given by

$$\epsilon_j(\omega) = \frac{f_j}{(\omega_j^2 - \omega^2) - i\Gamma_j\omega}. \tag{4}$$

In Fig. 3, we show transitions T_{VV} between valence bands V_1 and V_2, and transitions T_{vc} between valence and conduction bands V_2 and C. Interband transitions T_{vv} are adequately described by a single Lorentz oscillator with frequency $\hbar\omega = E_{v_1} - E_{v_2}$, that is, their contribution to ϵ_{inter} is $\epsilon_j(\omega)$ given by eqn. (4). The transitions T_{vc} cannot be so simply described because of their sharp, low-energy threshold E_T imposed by the position of the Fermi level. A group of narrow, overlapping oscillators with a fixed width (Γ) and frequency-dependent oscillator strength $f = A\omega^{1/2}$, was used to describe these transitions. Their contribution ϵ_T to the dielectric constant is

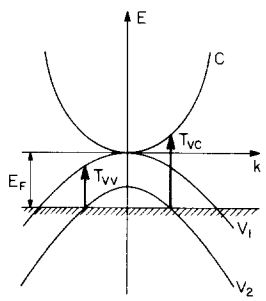

Fig. 3. Interband transitions T_{vv} and T_{vc}. Transitions T_{vv} are between roughly parallel valence bands V_1 and V_2 and are well described by a single Lorentz oscillator. Transitions T_{vc}, between the valence band V_2 and conduction band C have a low energy threshold and are described by a group of narrow oscillators (*cf.* eqn. (5)). This threshold energy can be used to locate the Fermi level.

$$\epsilon_T(\omega) = \begin{cases} \sum_m \dfrac{A(\omega_m - \omega_L)^{1/2}}{(\omega_m{}^2 - \omega^2) - i\Gamma\omega}, E_T < \omega < E_U \\ 0, \text{otherwise} \end{cases} \quad (5)$$

where A is a constant, and E_T and E_U are the threshold and cut-off energies in the absorption band. We should also mention that because we employ a superposition of Lorentz oscillators the Kramers–Kronig relationship between ϵ_1 and ϵ_2 is automatically satisfied. Finally, the total interband contribution can be written as

$$\epsilon_{inter} = \sum_j \epsilon_j(\omega_j, \Gamma_j, f_j) + \epsilon_T(A, E_T, E_U). \quad (6)$$

The parameters indicated in parentheses are adjusted to fit the data. The spectral features associated with the interband transitions were usually well separated in energy and can be fitted, for the most part, with minimal interference from parameters describing other transitions.

To calibrate our fitting procedure, we first analyzed the reflectance spectrum of pristine graphite using our model. For pristine graphite a threshold-type transition term was not needed. The trace at the bottom of Fig. 4 shows our data (HOPG) and our calculated reflectance (solid line). The fit is seen to be excellent. We also show the corresponding imaginary part of the dielectric constant plotted *vs.* energy in Fig. 5. As can be seen from the Fig-

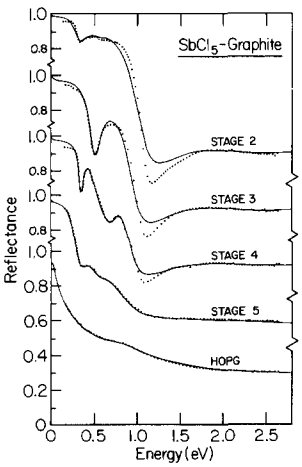

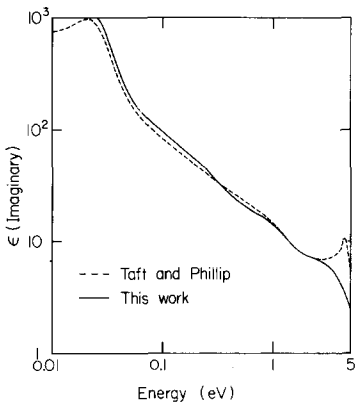

Fig. 4. Reflectance spectra of stage 2 - 5 $SbCl_5$–graphite and HOPG. The structures associated with interband transitions were all modeled as individual Lorentz oscillators (eqn. (4)). An interband transition term of the form given by eqn. (5) was *not* used in the fits (solid lines) shown in this Figure. This latter term models transitions with a sharp threshold for absorption. However, the calculated reflectance spectra of Fig. 6(a) - (c) were made incorporating this term into the dielectric constant.

Fig. 5. $\epsilon_2(\omega)$ *vs.* $\hbar\omega$ for HOPG. Calculated values in terms of our phenomenological, dielectric constant model are represented by the solid line. Values for $\epsilon_2(\omega)$ determined by Taft and Phillip (1965) using a Kramers–Kronig analysis are shown as a dashed line.

ure, our calculated values for $\epsilon_2(\omega)$ (solid line) are in good agreement with those obtained by Taft and Phillip [14] using a Kramers–Kronig analysis. The difference between the curves near 5 eV is due to the fact that the 5 eV transitions were represented by a contribution to the core dielectric constant. Thus, good agreement only up to ~2 eV would be expected.

The best fit to the reflectance data then requires an optimal adjustment of both the Drude and interband parameters in the phenomenological, dielectric-constant expression described in eqns. (2) - (6). The final choice of these parameters must also be consistent with the experimentally determined values of the dielectric constant measured at 1.96 eV. The agreement between the calculated and measured values of $\epsilon = \epsilon_1 + i\epsilon_2$ at 1.96 eV can be seen in Table 1.

4. Discussion of results

Reasonably successful attempts to fit the reflectance data of stages 2 - 5 $SbCl_5$–graphite were made using discrete Lorentz oscillators to describe the interband transitions. These results were reported earlier [15] and are shown in Fig. 4. As can be seen from the Figure the agreement between the calculated reflectance (solid curve) and the data is quite good for HOPG and the stage 5 compound. However, for stages 2, 3, 4 there is noticeable disagreement at the position of the reflectance minimum, which is located near the value of the screened plasma frequency. Motivated by the recent papers of Blinowski *et al.* [6], and Blinowski and Rigaux [7], we again analyzed the data, adding an absorption band due to interband transitions having a threshold energy E_T with a simple $\sqrt{\omega}$-dependence for $\epsilon_2(\omega)$. This band is determined by three parameters E_T, E_u and A as shown in eqn. (5). We arbitrarily employed a value of $E_u = 3.5$ eV for the high energy cut-off. The width and spacing of the overlapping oscillators in this band were fixed at 0.2 and 0.1 eV, respectively.

The addition of one of these $\sqrt{\omega}$-bands to each of the stages 2, 3, and 4 fits improved the agreement with the experimental data substantially. The improvement can be seen in Figs. 6(a), (b), (c), and (d). The values for the

TABLE 1

Comparison of calculated and measured values of the dielectric constant at $\hbar\omega = 1.96$ eV for graphite–$SbCl_5$

Stage No.	ϵ_1		ϵ_2	
	Meas.	Calc.	Meas.	Calc.
2	4.2 ± 0.3	4.4	4.3 ± 0.1	4.3
3	3.7 ± 0.4	4.0	5.1 ± 0.1	5.0
4	4.3 ± 0.6	4.3	5.5 ± 0.1	5.6
5	4.5 ± 0.5	4.3	6.5 ± 0.1	6.5
∞ (HOPG)	3.9 ± 0.7	4.0	7.8 ± 0.2	7.7

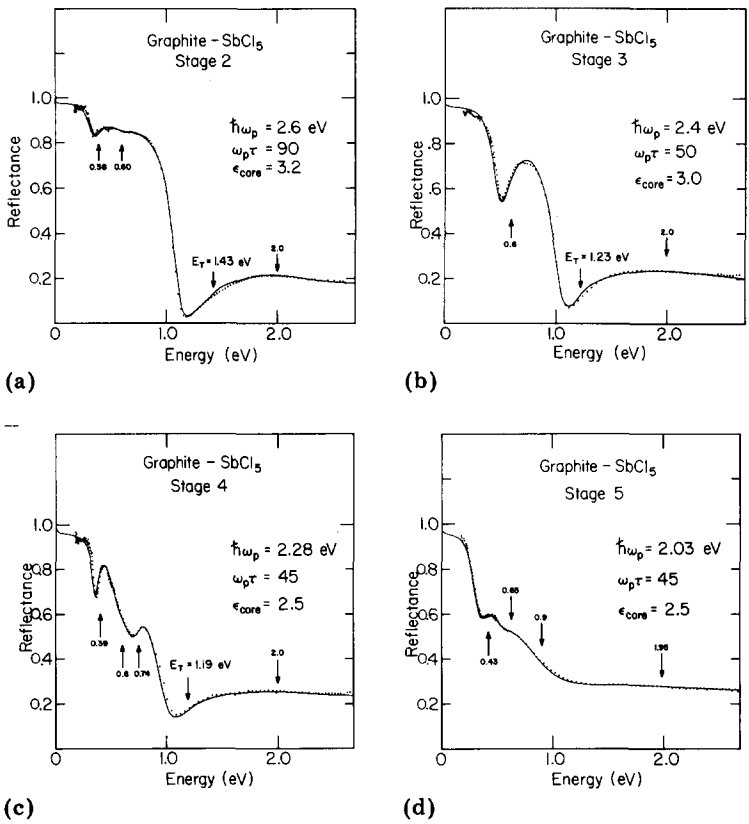

Fig. 6. (a) - (d). Absolute reflectance of stage 2 - 5 $SbCl_5$–graphite. The data are represented by the dots, the solid lines represent values calculated from our phenomenological, dielectric constant model. The interband transitions were described by the expression given by eqn. (6).

phenomenological dielectric constant parameters of stages 2 - 5 $SbCl_5$–graphite are given in Table 2(A) and 2(B); Table 2(A) contains the information regarding the free carrier and core dielectric constant parameters, while information concerning the interband transitions can be found in Table 2(B).

The behavior of the unscreened plasma frequency $\omega_p{}^2 = (4\pi Ne^2/m^*_{opt})$ with reciprocal stage $(1/n)$ is shown in Fig. 7. The data exhibit and approximately linear relation for $n = \infty$ (HOPG) up to $n = 4$, suggesting that the optical mass and the fractional ionization (of intercalated molecules) are, to a reasonable approximation, independent of stage in dilute compounds. For increasingly lower stages of intercalation the curve begins to saturate. We were unable to prepare a good quality stage 1 sample, which unfortunately prevents us from knowing whether the plasma frequency is a maximum for a stage 1 or a stage 2 compound. Most of the previous reflectance work by other workers has found the highest unscreened plasma frequency in the stage 1 compound. A noteable exception, however, was reported for AsF_5–graphite

TABLE 2(A)

Free carrier and core parameters in graphite–$SbCl_5$

	Stage				
	2	3	4	5	HOPG
ϵ_{core}	3.2	3.0	2.5	2.5	2.5
$\hbar\omega_p$ (eV)	2.60	2.40	2.28	2.03	0.44
$\omega_p\tau$	90	50	45	45	130
σ_{opt} $((m\Omega\ cm)^{-1})$	31.3	16.1	13.7	12.2	7.7

TABLE 2(B)

Parameters for interband transitions in graphite–$SbCl_5$

	Stage				
	2	3	4	5	HOPG
$\hbar\omega_1$ (eV)	0.38		0.39	0.43	0.023
Γ_1 (eV)	0.17	–	0.07	0.23	0.02
f_1	1.52		0.65	1.5	0.5
$\hbar\omega_2$	0.60	0.60	0.60	0.65	0.18
Γ_2	0.35	0.21	0.30	0.37	0.55
f_2	0.6	2.2	0.85	1.6	5.3
$\hbar\omega_3$			0.75	0.90	0.87
Γ_3	–	–	0.18	1.10	1.05
f_3			0.7	2.9	7.7
$\hbar\omega_4$	2.00	2.00	2.00	1.95	1.90
Γ_4	0.70	1.20	1.75	2.10	2.60
f_4	2.0	3.8	8.5	13.0	15.0
$\hbar\omega_5$			3.5	3.50	3.5
Γ_5	–	–	2.25	3.50	3.5
f_5			13.0	47.0	52
E_T (eV)	1.43	1.23	1.19		
E_C (eV)	3.50	3.50	3.50	–	–
A	0.25	0.25	0.18		

[5] where they found a stage 2 unscreened plasma frequency $\omega_p(2) = 4.04$ eV which is greater than their reported value of $\omega_p(1) = 3.39$ eV for the stage 1 compound. This result (*i.e.*, $\omega_p(2) > \omega_p(1)$) may be either due to an artifact of the analysis in which they model the interband transitions as a frequency independent constant, or due to an artificially high ϵ_{core} for the stage 2 compound. Our choice for ϵ_{core} must be consistent with the additional constraint at the 1.96 eV calibration points for ϵ_1 and ϵ_2 (see Table 1).

Values for the optical conductivity $\sigma_{opt} = \omega_p{}^2\tau/4\pi$ increase from a value of 1.2×10^4 $(\Omega\ cm)^{-1}$ for a stage 5 compound to a value of 3.1×10^4

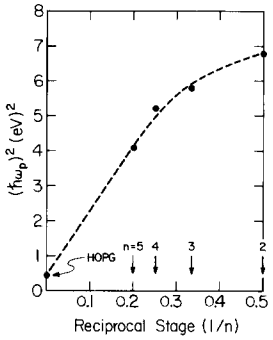

Fig. 7. $\omega_p{}^2 = (4\pi Ne^2/m^*)$ *vs.* reciprocal stage $(1/n)$ for stage 2 - 5 $SbCl_5$–graphite and HOPG ($n = \infty$). The dashed line is a guide for the eye.

$(\Omega\ \text{cm})^{-1}$ for a stage 2 compound; σ_{opt} (HOPG) = 0.8×10^4 $(\Omega\ \text{cm})^{-1}$. This represents a factor of ~4 increase for σ_{opt} from stage ∞(HOPG) to a stage 2 compound. Noting that the d.c. conductivity of copper (300 K) is a factor of ~23 higher than graphite (300 K), the optical conductivity data can then be loosely interpreted to suggest that the d.c. conductivity of stage 2 $SbCl_5$–graphite ~1/6 that of copper or comparable with chromium. That being the case, then one would find $\sigma_{opt} \sim (1/2)\sigma_{d.c.}$ for stage 2 $SbCl_5$–graphite.

We now consider the structure in the reflectance spectra associated with interband transitions. Parameters describing this structure are summarized in Table 2(B). The values for the various frequencies found in the Table can be correlated with the various critical points in the joint optical density of states of these compounds, and thus should be useful in determining the correct band model. Our analysis of the low energy region (0.1 - 3.0 eV) *via* the complete dielectric constant expression, eqns. (2) - (6), offers information not only about the correct position of these critical points, but also yields their relative oscillator strengths. The actual frequency of a transition need not correspond to the spectral position of the associated peak, dip, or shoulder, in the reflectance curve, but can be significantly shifted due to the presence of other contributions to the complex dielectric constant. These shifts are most apparent in the stage 3 and 4 spectra shown in Fig. 6(b) and (c), where the arrows indicate the transition energies.

We now turn our attention to the interband transitions found in the stage 2 compound and discuss them in terms of the recently available band models. In agreement with the data of several stage 2 acceptor compounds (Br_2, ICl) [6] we find structure at 0.38 eV. Interband transitions at these energies have been predicted by Blinowski *et al.* [6] and, according to their band model, these transitions are between valence bands. They also predict interband transitions with a threshold energy = $2E_F$ between the highest lying valence band and its mirror image conduction band. We find a threshold energy at E_T = 1.43 eV, which would place the Fermi energy 0.71 eV below the top of the higher lying valence band in their model. The 0.38 eV transitions and the threshold energy E_T = 1.43 eV are clearly evident in Fig. 8 where we show calculated values of $\epsilon_2(\omega)$ used in fitting the stage 2 re-

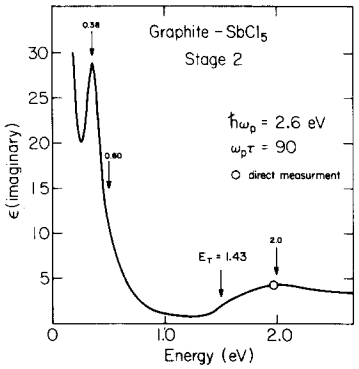

Fig. 8. Calculated values of $\epsilon_2(\omega)$ for stage 2 $SbCl_5$–graphite which corresponds to the fit (solid line) shown in Fig. 6(a). The arrow at E_T = 1.43 eV marks the value of the low energy threshold for interband transitions from states at the Fermi level to empty states in the higher lying band(s). The other arrows locate the energies of single Lorentz oscillators used in fitting the reflectance spectrum.

flectance spectra. The analysis of the stage 2 spectra also reveals interband transitions at 0.60 eV which cannot be explained by their quasi 2D band model. The 3D band model for a stage 2 compound proposed by Dresselhaus and Leung does not contain bands with mirror symmetry, and, depending on the position of the Fermi level, may be able to account for interband structure at 0.38, 0.60 and 1.43 eV. This remains to be seen after they present further quantitative information concerning their bands. We also should point out another significant difference between these two band models for stage 2 compounds. The band model of Dresselhaus and Leung has *c*-axis dispersion which opens up additional small energy differences between the valence bands and between the conduction bands of the order of ~0.1 eV. Thus, depending on the strength of the matrix elements for these low-energy transitions they would predict structure in the infrared at ~800 cm^{-1}. These low energy transitions are not predicted by the stage 2 band model of Blinowski *et al.* [6].

We now turn our attention to the higher stage (n = 3, 4, 5) $SbCl_5$–graphite interband transitions. In the stage 3 compound we find transitions at 0.60 and 2.00 eV in addition to a group of transitions with a threshold energy E_T = 1.23 eV. According to Blinowski and Rigaux [7] optical transitions between mirror valence and conduction bands would have a threshold energy $E_T = 2E_F$, thus, in their model the stage 3 Fermi level for $SbCl_5$–graphite is ~0.61 eV below the line of reflection symmetry of their band structure. They have calculated this value to be ~0.5 eV for stages 3 and 4. We also note that they expect transitions between valence bands in the stage 3 compound at ~0.55 eV, in good agreement with the observed structure in our spectra at 0.6 eV.

In the stage 4 and 5 compounds of $SbCl_5$–graphite we observe many transitions which are listed in Table 2(B). A threshold-type group of interband transitions was not needed to fit the stage 5 spectrum. For stage 4 we

find E_T = 1.19 eV which, in a mirror band model, places the Fermi level at ~0.60 eV below the line of reflection symmetry.

5. Conclusion

We have examined the optical reflectance of stages 2 - 5 $SbCl_5$–graphite in the photon energy range 0.1 - 3.0 eV. Our analysis of these spectra in terms of a phenomenological, dielectric-constant model has identified structure associated with interband and intraband transitions. Our data appear to be in reasonably good agreement with the quasi-2D band models of Blinowski *et al.* [6, 7]. A recent competing 3D band model for stage 1 - 7 compounds suggested by Dresselhaus and Leung [8] needs to be considered in the light of our data.

A more detailed discussion of these competing band models in terms of the data reported herein will be published later.

Acknowledgments

We thank Professor C. Brock for her assistance with the X-ray characterization of the samples. The X-ray equipment was purchased, in part, under an NSF (Chemistry) equipment grant. We also are grateful to Dr. A. W. Moore for his generous gift of the HOPG. This work was supported, in part, by the Research Corporation.

References

1 L. R. Hanlon, E. R. Falardeau and J. E. Fischer, *Mater. Sci. Eng., 31* (1977) 161.
2 J. E. Fischer, T. E. Thompson, G. M. T. Foley, D. Guérard, M. Hoke and F. L. Lederman, *Phys. Rev. Lett., 37* (1976) 769.
3 M. Zanini and J. E. Fischer, *Mater. Sci. Eng., 31* (1977) 169.
4 D. Guérard, G. M. T. Foley, M. Zanini and J. E. Fischer, *Nuovo Cimento, 38B* (1977) 410.
5 L. R. Hanlon, E. R. Falardeau and J. E. Fischer, *Solid State Commun., 24* (1977) 377.
6 J. Blinowski, N. Hau, C. Rigaux, J. P. Viereu, R. Le Toullec, G. Furdin, A. Hérold and J. Mélin, *J. Phys. (Paris), 41* (1980) 47.
7 J. Blinowski and C. Rigaux, *J. Phys. (Paris), 41* (1980) 667.
8 G. Dresselhaus, S. Y. Leung and M. Shayegan, *Bull. Am. Phys. Soc., 25* (1980) 298.
9 V. R. K. Murthy, D. S. Smith and P. C. Eklund, *Mater. Sci. Eng., 45* (1980) 77.
10 D. S. Smith, *Ph.D. Thesis*, University of Kentucky, unpublished.
11 J. Mélin and A. Hérold, *C. R. Acad. Sci., 269* (1969) 877.
12 J. Mélin and A. Hérold, *Carbon, 13* (1975) 357.
13 P. C. Eklund, V. R. K. Murthy and S. Leung, *Synth. Met., 2* (1980) 99.
14 E. A. Taft and H. R. Phillip, *Phys. Rev., 138* (1965) A 197.
15 D. S. Smith, V. R. K. Murthy and P. C. Eklund, *Bull. Am. Phys. Soc., 25* (1980) 336.